Single-Crystal Elastic Moduli and the hcp → bcc Transformation in Ti, Zr, and Hf

E. S. FISHER AND C. J. RENKEN
Argonne National Laboratory, Argonne, Illinois
(Received 24 February 1964)

The variations with temperature of the elastic moduli in single crystals of hcp Ti, Zr, and Hf have been experimentally determined from 4°K up to 1155°K, using an ultrasonic wave interference technique. The c_{11}, c_{33}, and c_{44} differ considerably among the three metals, whereas the c_{66} shear moduli for Ti and Zr are similar to within 1% between 4 and 300°K and less than 10% at 1100°K. There is very marked anisotropy in the temperature dependence of the shear moduli in Ti and Zr, c_{66} decreasing by 75% between 4 and 1100°K whereas c_{44} decreases by 40%. A very pronounced deviation from a linear temperature dependence of c_{66} occurs at a temperature which coincides with the anomalous curvatures in the published electrical resistivity data. The relatively small c_{66} shear moduli at the hcp → bcc phase transformation temperatures are as expected from the transformation shear mechanisms suggested by Burger. A survey of existing elastic modulus and thermal expansion data in hcp metals leads to the conclusion that a relatively high temperature dependence in c_{66} and the occurrence of hcp → bcc transformations are characteristic of metals with $c/a<1.60$. It is suggested that these characteristics are due to the transverse thermal vibrations in the basal planes, and that the transformation results from anharmonic contributions to the free energy which are indicated by specific heat data. Contrary to comparison in other hcp metals, the Debye θ from 4°K elastic moduli in Ti, Zr, and Hf are in excellent agreement with published specific heat data. A slight anomaly at 18°K in Ti is indicated which may be associated with published resistivity minima in Ti alloys.

AMONG the large number of pure metals and alloys which crystallize in the bcc structure but transform to hcp or other noncubic structures upon cooling, there are two groups in which the relative stabilities of the bcc phases and the transformation mechanisms seem to be qualitatively understood on the basis of the anisotropy in the bcc elastic shear moduli, or shear anisotropy. These include the alkali metals Li, Na and the Li-Mg alloys in one group and the β-brass type alloys, including Au-Cd, in another. The elastic moduli of single crystals[1–4] are consistent with Zener's suggestion[5] that the bcc structures are stable relative to the low-temperature structures because of the high vibrational entropy associated with the relatively small $\{110\}\langle 110\rangle$ shear moduli, $\frac{1}{2}(c_{11}-c_{12})$. All of these metals and alloys have high anisotropy ratios, defined as $2c_{44}/(c_{11}-c_{12})$. The mechanisms of the martensitic transformations in these metals also can be qualitatively explained on the basis of the shear anisotropy. Because of the relatively small $\frac{1}{2}(c_{11}-c_{12})$, the predicted mechanism for the primary shear during transformation would be $\{110\}\langle 110\rangle$ of the bcc structure; the habit planes determined by various means for the above transformations[6] are indeed close to $\{110\}$ planes, thus suggesting that $\{110\}\langle 110\rangle$ shears are involved in the mechanisms.

There are, however, several difficulties which arise when attempting to understand the relative stabilities of all the bcc structures and their transformation mechanisms in terms of their high anisotropy ratio, or small $\frac{1}{2}(c_{11}-c_{12})$. The most prominent example is the consistency of the habit-plane studies in Ti and Zr which indicate that these bcc → hcp transformations involve $\{112\}\langle 111\rangle$ shears in the bcc phase.[7,8] This also is the mechanism expected from the lattice relationships of the bcc and hcp structures proposed by Burger.[7] Burgers' relationship indicates that the shear anisotropy in these bcc structures is considerably different, since the preference for $\{112\}\langle 111\rangle$ shear indicates an isotropic shear modulus ratio (see Appendix for explanation). Since the stable bcc transition metals V, Cr, Nb, Mo, Ta, and W, are nearly isotropic in this respect, it would not be entirely surprising to find similar properties in bcc Ti, Zr and other transitional metals. Zener's theory for the relative stability of the high-temperature bcc phases would seem then not to apply to these metals unless the vibrational entropies of the hcp structures have unusual temperature dependence near their temperatures of transformation.

In the present experiments the elastic moduli of hcp Ti and Zr were measured over a temperature range from 4°K to respective phase transformations, 1155 and 1135°K. The elastic moduli of Hf were measured from 4°K to above 300°K. The results indicate that anisotropy in the temperature dependence of the hcp shear moduli is closely related to the hcp → bcc phase transformations. Lattice specific heat calculations suggest that this relationship is due to high-temperature anharmonicity in the thermal vibrations.

MEASURING PROCEDURES

Wave Velocity Measurements

The elastic moduli were determined from measurements of acoustic wave velocities propagated in three

[1] J. Trivisonno and C. S. Smith, Acta Met. **9**, 1064 (1961).
[2] W. B. Daniels, Phys. Rev. **119**, 1246 (1960).
[3] G. McManus, Phys. Rev. **129**, 2004 (1963).
[4] S. Zirinsky, Acta Met. **4**, 164 (1956).
[5] C. Zener, *Elasticity and Anelasticity of Metals* (University of Chicago Press, Chicago, 1948).
[6] J. S. Bowles, Trans. AIME **191**, 44 (1951).
[7] W. G. Burgers, Physica **1**, 561 (1934).
[8] A. J. Williams, R. W. Cahn, and C. S. Barrett, Acta Met. **2**, 117 (1954).

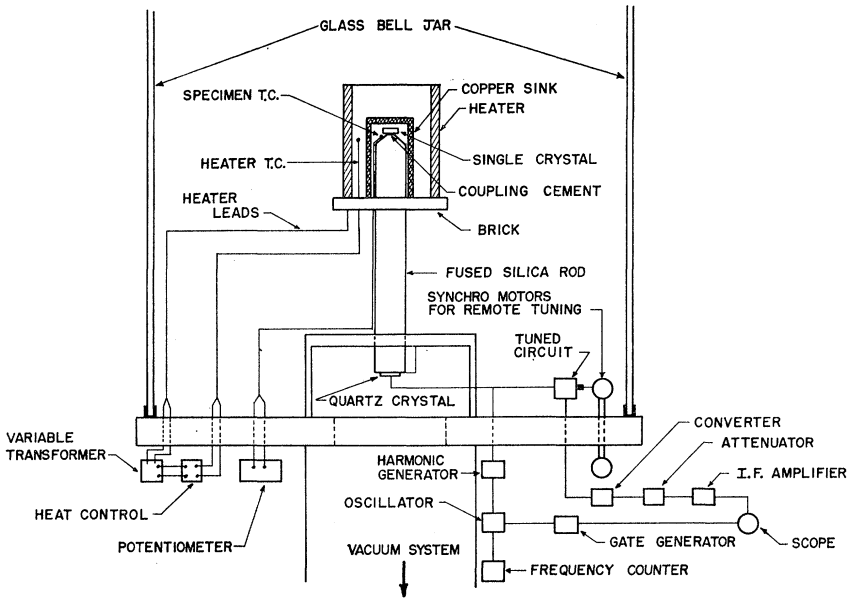

FIG. 1. Arrangement of apparatus for measuring temperature dependence of ultrasonic wave velocities above 300°K.

different crystallographic directions of the hcp crystals. The relations for computing the five fundamental elastic moduli from the measured wave velocities are given in Table I. The wave velocities were measured by the phase comparison technique developed by McSkimin.[9] Pulsed trains of high-frequency ultrasonic waves were propagated along a path consisting of a fused or crystal quartz rod and the specimen, which were acoustically coupled by a suitable cement. The wave velocity was derived from the relation

$$V=\frac{2tf_0}{n+\gamma/360}, \tag{1}$$

where f_0 is the wave frequency at which there are an integral number of half-wavelengths in the specimen path, t is the path length in the specimen, n is the integer corresponding to the number of waves in 2 t, and γ is the angle in degrees associated with the phase shift in the coupling cement. Details of the method for determining f_0, n, and γ are given in Ref. 9.

During the absolute wave velocity measurements, the specimens were maintained at a constant temperature (293 or 298°K) by controlling the temperature of water flowing through the hollow wall of a metal jacket surrounding the buffer rod and specimen.

Variation with temperature above 300°K. The physical arrangement schematically shown in Fig. 1 was used to measure the variation of the wave velocities with temperatures above 300°K. The essential components were (1) the cylindrical buffer rod of 18 mm diam made from optical quality fused silica, (2) the piezoelectric quartz transducer (20-Mc/sec X cut for compressional waves, or 13-Mc/sec Y cut for shear waves) which was coupled to the flat end of the buffer rod by soft solder on silver paste, and (3) the single-crystal specimen consisting of two flat and parallel faces, one of which was coupled to the buffer rod by a quasi-water-glass cement described in Ref. 10.

The buffer rod was supported vertically in a table on the base plate of a 45-cm (18-in.) glass vacuum bell jar unit. A nichrome wire furnace supplied the heat to the specimen which was surrounded by a copper heat sink. The maximum pressure during a run in which the specimen temperature approached 1300°K was about 5×10^{-5} Torr.

The rf pulses of known frequency (ranging from 35 to 50 Mc/sec) from an outside generating and detecting

TABLE I. Relations between acoustic wave velocities and elastic stiffness moduli in hcp crystals.

Direction of wave propagation relative to c axis	Type mode	Direction of particle motion	Equation for ρV^{2}[a]
0°	longitudinal	00l	c_{33}
	shear	hk0	c_{44}
90°	longitudinal	hk0	c_{11}
	shear	$h'k'$0	$\frac{1}{2}(c_{11}-c_{12})=c_{66}$
	shear	00l	c_{44}
Intermediate	quasilongitudinal	hkl	(ρV_{QL}^2)[b]
	quasishear	$h'k'l$	(ρV_{QS}^2)[c]
	shear	$h'k'$0	(ρV_{PS}^2)[d]

[a] ρ = density, V = wave velocity.
[b] $2\rho V_{QL}^2=c_{33}C^2+c_{11}S^2+c_{44}+\{[c_{11}S^2-c_{33}C^2+c_{44}(C^2-S^2)]^2+4C^2S^2(c_{13}+c_{44})^2\}^{1/2}$.
[c] $2\rho V_{QS}^2=c_{33}C^2+c_{11}S^2+c_{44}-\{[c_{11}S^2-c_{33}C^2+c_{44}(C^2-S^2)]^2+4C^2S^2(c_{13}+c_{44})^2\}^{1/2}$.
[d] $\rho V_{PS}^2=c_{44}C^2+\frac{1}{2}(c_{11}-c_{12})S^2$. C = cosine angle between wave propagation direction and c axis. S = sine angle between wave propagation direction and c axis.

[9] H. J. McSkimin, IRE Trans. Ultrasonics Eng. **25**, P.G.U.E.-5 (1957).

[10] E. S. Fisher and C. J. Renken, J. Acoust. Soc. Am. **35**, 1005 (1963).

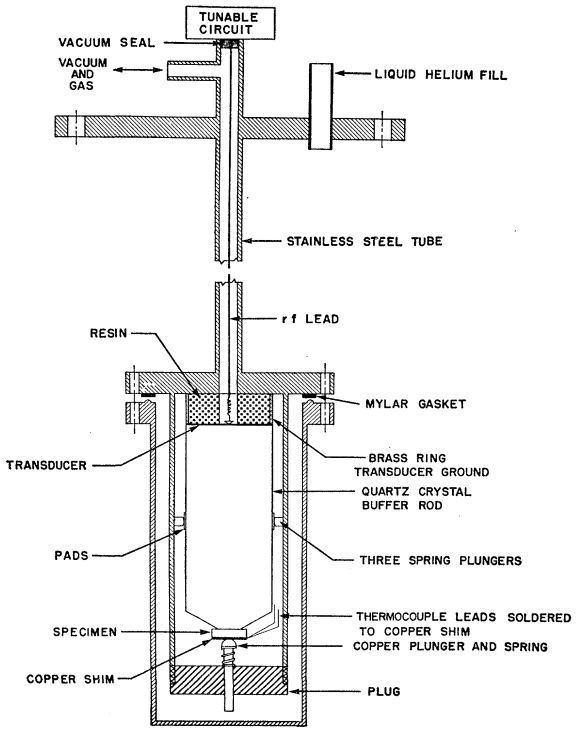

FIG. 2. Schematic drawing of low-temperature buffer rod unit.

system, described in Ref. 11, passed through the base plate to the transducer. The reflected waves were picked up by the transducer and passed through a tunable circuit inside of the bell jar to the converter and amplifier sections outside of the bell jar. The variable capacitor in the inside circuit was operated by remote control using two synchronous motors.

The variation of wave velocity with temperature was obtained by observing the change in f_0, of Eq. (1), for a constant n, giving the following relation:

$$\frac{V_T}{V}=\frac{t_T}{t}\frac{(f_0)_T}{f_0}\frac{n+\gamma/360}{n+\gamma_T/360}, \tag{2}$$

where V, t, f_0, and γ are the variables at the reference temperature. The specimen thickness was determined from available thermal expansion data as explained in detail below. The major variable $(f_0)_T$ was measured on a Hewlett Packard 524C frequency counter. The method of evaluating γ_T is explained in Appendix B of Ref. 9.

Temperature measurements were made using chromel-alumel thermocouples, with hot junctions in contact with a beveled face of the buffer rod, as shown in Fig. 1. Direct contact with the specimen was not practical because of the brittle character of the coupling cement. Even though the thermocouple hot junctions were only $\frac{1}{16}$ in. distant from the specimen, the thermal gradient along the buffer rod was a source of significant error for heating rates above 1°/min in the range of 330–700°K (below the range of heating by radiation).

Limitations of coupling cement. Although only seven runs are necessary to completely determine the elastic moduli and internal consistency of data for crystals of hexagonal symmetry, the data presented here required considerably more runs because of interruptions by breakage of the acoustic coupling cement. The preparation of the quasi-water-glass cement and other details pertaining to optimum conditions for its use are given in Ref. 10. It should be noted here, however, that the successful use of this cement above 600°K was extremely sensitive to its chemical composition and to the condition of the metal surface. Fifteen runs were needed to complete the Zr data given here, 25 runs were required for Ti, and only one set of Hf measurements were extended above 300°K.

Low-temperature apparatus. For measurements below room temperature, the specimen and buffer rod assembly, including the transducer, were lowered into a 100-cm-high inner Dewar of a glass cryostat. A diagram of the measuring apparatus is shown in Fig. 2. Because of the drastic increase in ultrasonic attenuation in fused silica below 273°K, the buffer rods were made from cylindrical quartz crystals, 2.5 cm in diameter by 7.5 cm long. For propagation of longitudinal waves, a 20-Mc/sec X-cut transducer was soldered to the flat end of a quartz crystal in which the cylindrical axis was parallel to the X direction. An AC-cut quartz cylinder was used for shear wave propagation with a 13-Mc/sec Y-cut transducer soldered to it so that the [100] directions in the Y cut and AC cut were parallel. The circuitry was similar to that used in the high-temperature apparatus, except that the tuning outside of the converter section was carried out about 75 cm from the transducer, just above the top flange of the cryostat. The measured frequencies ranged from 35 to 50 Mc/sec. The buffer rod assembly was enclosed in a copper can which provided a vacuum-tight enclosure to prevent frosting on the rf contacts and to reduce the frequency of temperature fluctuations.

Temperatures between 78 and 46°K were attained by pumping on liquid nitrogen, and the data were checked against that obtained by slow warming from liquid-helium temperatures. Temperatures of 2°K were obtained by pumping on the liquid helium. Data between 78 and 300°K were obtained during slow warming. Because of the relatively small temperature coefficients of the elastic moduli below 77°K, temperature measurements of ±1°K were considered sufficiently accurate; consequently, a K-3 potentiometer and a copper-constantan thermocouple, calibrated periodically against vapor pressure measurements above liquid and solid nitrogen and liquid helium, were used for all temperature measurements.

[11] C. J. Renken, Argonne National Laboratory Report ANL-6280, 1959 (unpublished).

There were no problems encountered in maintaining acoustic coupling with either Nonaq stopcock grease or Dow Corning 200 silicone oil (2.5×10^6 centapoise). This simplified the problem of making thermal contact between the thermocouple and specimen; a copper shim soldered to the welded tip of the thermocouple was clamped to the specimen by a spring plunger. The temperature gradients were, however, large enough to create significant errors in temperature measurement unless sufficient time was permitted to attain a steady-state condition.

Specimen Preparation

The procedure for preparing the plate shaped specimens is given in Ref. 12. The crystal orientations were established within maximum errors of $\pm30'$.

Zr. The procedure for obtaining the Zr single crystals is described in Ref. 13. Measurements were carried out on six different specimens, with thicknesses of 2.5–5 mm. Two were oriented for wave propagation 90° to the [001] axis, two for propagation at $47°\pm15'$ (as determined by the x-ray diffractometer method given in Ref. 12) to the [001], and two for propagation 0° to [001]. One set was used for both high- and low-temperature measurements, and the second set was used to determine whether possible contamination by gases during the high-temperature runs of the first set had changed the absolute values at 300°K, or the temperature coefficients below 300°K.

Ti. Three Ti single crystals were prepared from one 45-cm-long rod of iodide crystal bar which was subjected to four passes in a floating zone melting apparatus. One crystal of reasonably good structural perfection was cut directly from the zone-refined rod. Two others were obtained from zone-refined rods subjected to the phase change-anneal process using the same annealing procedures described in Ref. 13. The crystals were subsequently ground to form three single crystal plates with faces respectively normal, parallel, and inclined $44°\pm15'$ to the (001) plane. These crystals were from 2 to 3 mm thick and about 6 mm in lateral dimensions.

Hf. Single crystals of Hf were obtained from an electron-beam-refined button donated by the U. S. Bureau of Mines, Albany, Oregon. This button was annealed for 24 h at 1920°K and contained a number of relatively large and structurally close to perfect grains after cooling. The crystals contained 4.1 wt % Zr, 0.01% oxygen, and trace amounts of other impurities adding up to 0.01%.

The Hf studies were carried out with two Hf single crystals, one of which was ground to form two sets of parallel faces for wave propagation parallel and 90° to the [001] direction. The other crystal was ground to form two parallel faces inclinded $64°\ 18'\pm10'$ to the (001) plane.

Limits of Measurements

Because of high acoustic wave attenuation in the specimens or because of coupling difficulties, the data obtained were not sufficient to compute all of the elastic moduli at the respective temperatures of the hcp to bcc phase transformations.

Zr. In the case of the Zr data, difficulties were encountered due to significant increases in wave attenuation within the specimen. The attenuation was most pronounced for the c_{44} wave modes, where the wave interference began to weaken at about 1060°K and became too weak for reproducible measurements above 1080°K. The c_{11} mode was by far the least affected, and measurements were completed up to 1133°K. For c_{66}, c_{33}, ρV_{QL}^2, and ρV_{QS}^2 the maximum temperatures of the measurements are in the range of 1105–1125°K.

In all the experiments, heating was continued to 20 or 30°K above the transformation temperature (1135°K). In no case was it possible to detect wave interference above 1133°K. Upon cooling, however, the interference reappeared about the same temperatures at which disappearance occurred during the heating cycle. There was no evidence of a permanent increase in attenuation or orientation change. Some specimens were thermally cycled from 950 to 1150°K as many as ten times. Some evidence of structural damage was detected in the broadening of the peak intensities for certain principal x-ray reflections.

Ti. The increase in acoustic wave attenuation upon approaching the transformation temperature of Ti, (1155°K) was much less than in Zr. The occurrence was, however, similar in that the shear modes were most affected, whereas, the c_{11} mode for Ti was totally unaffected until transformation occurred. None of the measurements failed to reach 1155°K because of excessive attenuation. The measurements for the c_{33} mode were interrupted because of an equipment failure at 1083°K. Several subsequent attempts to complete the data ran into coupling failures. The measurements of the wave velocity for the quasilongitudinal mode (44° propagation direction) were not completed because of repeated failures of the coupling when using the quasi-water glass at or below 600°K. A run was then made using an epoxy phenolic coupling cement, described in Ref. 10, which furnished data up to 925°K. Since the velocity of this wave mode is necessary only to determine the modulus c_{13} which is almost temperature independent in Zr and also in Ti up to 925°K, it seemed justified to extrapolate from the available data to obtain values above 925°K.

An interesting difference was noted between Zr and Ti in the behavior of the coupling during the phase transformation. Whereas the coupling did not break during thermal cycling through the 1135°K tempera-

[12] E. S. Fisher and H. J. McSkimin, J. Appl. Phys. **29**, 1473 (1958).
[13] E. S. Fisher and C. J. Renken, J. Nucl. Mater. **4**, 311 (1961).

ture range with Zr, as indicated by the return of the wave interference upon cooling, the coupling apparently broke catastrophically during the first cycle of the Ti specimens, as indicated by complete absence of wave interference on cooling. No evidence of significant structural damage to the crystals by the phase transformation has been found.

Hf. There was no intention of reaching the temperature of the phase transformation of Hf. The immediate interest was to examine the anisotropy of the temperature coefficients for the shear moduli in a 300°K range of temperatures.

Densities and Thermal Expansion

The mass densities used for computing the absolute values of elastic moduli at reference temperatures are as follows:

$$\rho_{\mathrm{Ti}}=4.5063 \text{ g/cc at } 298^\circ\mathrm{K},$$
$$\rho_{\mathrm{Zr}}=6.505 \text{ g/cc at } 293^\circ\mathrm{K},$$
$$\rho(\mathrm{Hf}+4\%\ \mathrm{Zr})=12.727 \text{ g/cc at } 298^\circ\mathrm{K}.$$

The Ti and Zr densities are derived from the lattice parameter data of Willens[14] and of Swanson and Fuyat,[15] respectively. The density of the Hf crystals was computed from the lattice parameters of a sample of the alloy.[16] A mean atomic weight based on the relative quantities of hafnium and zirconium atoms was used in the calculation. A direct measurement of the density of one of the Hf single crystals, using a hydrostatic weighing technique, gave a density of 12.784 g/cc, indicating a possible error in the elastic moduli of $+0.45\%$ due to the error in the density.

The changes in lattice parameters with temperature are required not only to evaluate the thickness ratio t_T/t of Eq. (2), but also to compute the elastic moduli ρV^2, where ρ is the density of the specimen and V the wave velocity of Eq. (2). The following equations are then used to evaluate the elastic moduli $(\rho V^2)_T$ at a given temperature for crystals of hexagonal symmetry:

$$\frac{(\rho V^2)_T}{\rho V^2}=r^2\left(\frac{t_T}{t}\right)^2\frac{a^2c}{(a^2c)_T}, \text{ general} \tag{3}$$

$$=r^2\frac{c}{(c)_T}, \text{ for wave propagation 90° to [001]} \tag{3a}$$

$$=r^2\left[\frac{c}{(c)_T}\sin^4\theta+\left(\frac{a}{(a)_T}\right)^2\frac{(c)_T}{c}\cos^4\theta+\frac{a}{(a)_T}2\sin^2\theta\cos^2\theta\right], \tag{3b}$$

for wave propagation at angle θ to [001]

$$=r^2\left(\frac{a}{(a)_T}\right)^2\frac{(c)_T}{c},$$

for wave propagation parallel to [001], (3c)

where r is the corrected in-phase frequency ratio, $[(f_0)_T/f_0][n+\gamma/360]/[n+\gamma_T/360]$, a and c are the lattice parameters of the hexagonal unit cell, and $a^2c/(a^2c)_T$ is the density ratio ρ_T/ρ.

Specific information regarding the temperature dependence of a and c are available for Zr from 273°K to the phase-transformation temperature, 1135°K.[17,18] For Ti there is only one set of measurements available giving a and c between 298 and 920°K.[14] No measurements of the anisotropy of thermal expansion are available for Hf. There are, however, numerous measurements of thermal expansion in polycrystalline rods of all three metals which almost cover the temperature ranges of interest to the present work.[19–23] These data extend from about 75 to 1123°K. Since measurements of other properties, including the present $(f_0)_T/f_0$ values, indicate that no phase transitions occur below 75°K, it seems safe to assume that the error in extrapolation to 0°K from the measured thermal expansion is not significant with respect to the accuracy of other factors involved in computing ρV^2. These polycrystalline dilations can then be quite useful in estimating the changes in a and c in the temperature ranges where such values have not been measured, since the measured length changes in a randomly oriented polycrystal sample are related to the lattice parameters as follows:

$$\frac{l_T}{l}=\frac{1}{3}\left[2\frac{(a)_T}{a}+\frac{(c)_T}{c}\right]. \tag{4}$$

On the basis of careful analyses of all the thermal expansion data, the maximum changes in the ρV^2 values for zirconium and titanium due to specimen thickness and density changes between 300°K and the transformation temperatures are 0.95% and 1.53%, respectively. Between 300°K and 4°K an error of 50% in estimating thermal expansion would produce an error of 0.1% in the 4°K ρV^2 for all three metals.

RESULTS

Elastic Moduli and Cross Checks

Values at reference temperatures. The elastic moduli computed from absolute wave velocity measurements

[14] R. H. Willens, U. S. Air Force Office of Scientific Research Report AFOSR-1839, 1961 (unpublished).
[15] H. E. Swanson and R. K. Fuyat, Natl. Bur. Std. (U.S.) Circ. No. 539, Vol. 2, 11 (1953).
[16] E. S. Fisher and H. W. Knott (to be published).
[17] L. T. Lloyd, Argonne National Laboratory Report ANL-6591, 1963 (unpublished).
[18] G. B. Skinner and H. L. Johnston, J. Chem. Phys. **21**, 1383 (1953).
[19] C. F. Squire and A. R. Kaufman, J. Chem. Phys. **9**, 673 (1941).
[20] H. D. Erfling, Ann. Physik **34**, 136 (1939).
[21] P. Hidnert, J. Res. Natl. Bur. Std. **30**, 101 (1943).
[22] E. S. Greiner and W. C. Ellis, Trans. AIME **180**, 657 (1949).
[23] H. K. Adenstadt, Trans. Am. Soc. Metals **44**, 949 (1952).

TABLE II. Elastic moduli of titanium, zirconium, and hafnium at reference temperatures.

Direction of wave propagation relative to c axis	Equation for ρV^2	Measured ρV^2 (10^{12} dynes/cm^2) ($\pm 0.20\%$) Titanium (298°K)	Zirconium (293°K)	Hafnium (298°K)
0°	c_{33}	1.8070	1.649	1.9690
	c_{44}	0.4671	0.3207	0.5565
90°	c_{11}	1.6240	1.4350	1.8110
	c_{44}	0.4664	0.3207	0.5578
	c_{66}	0.3522	0.3548	0.5409
Intermediate[a]	ρV_{QL}^2	1.6780	1.4170	1.8111
	ρV_{QS}^2	0.5118	0.4418	0.5927
	ρV_{PS}^2	0.4108	0.3389	0.5239
Density (g/cc)		4.5063	6.5050	12.7270

[a] Intermediate propagation directions: Ti, 44°±15′; Zr, 46°50′±10′; Hf, 64°20′±15′.

are given in Table II. The reference temperatures are 293°K for Zr, and 298°K for both Ti and Hf.

The errors in the ρV^2 values due to errors in sample thickness and wave velocity measurements can be estimated from the internal checks given by classical elasticity theory, namely (1) a comparison of the c_{44} moduli determined from wave propagation parallel and perpendicular to the c axis, respectively, (2) a comparison of the observed ρV_{PS}^2, defined in Table I, with that computed from the two principal shear moduli and the orientation of the intermediate direction of wave propagation, and (3) a comparison of the two values for c_{13} determined from ρV_{QL}^2 and ρV_{QS}^2, respectively, according to the equations given below Table I. The differences observed in the above comparisons are given in Table III, expressed in percent of observed values, or mean values. The c_{44} and ρV_{PS}^2 comparisons range

TABLE III. Cross checks of absolute measurements.

	$\frac{\Delta c_{44}}{c_{44}}\times 100$ (%)	$\left(\frac{\rho V_{PS}^2 \text{ calc.-obs.}}{\text{obs.}}\right)\times 100$ (%)	c_{13} (10^{12} dynes/cm^2) from $\rho_{QL}{}^2$	from $\rho_{QS}{}^2$
Titanium	0.15	0.17	0.697 ±0.008	0.688 ±0.003
Zirconium	0.00	0.03	0.659 ±0.005	0.653 ±0.002
Hafnium	0.24	0.10	0.678 ±0.015	0.659 ±0.005

from 0.00% to a maximum deviation of 0.24%, indicating that the probable errors in the individual ρV^2 values, outside of the probable errors in density, can be safely assumed to be less than 0.2%. The probable errors in the c_{13} moduli are considerably greater than 0.2% because of accumulation of errors in the computation. The probable errors given for c_{13} are based on a probable error of 0.2% in each ρV^2 and 10′ errors in orientation of the intermediate directions of wave propagation. The weighted mean values of c_{13} fall within the range of each computed value, indicating again the validity of the assumed 0.2% probable error in each ρV^2.

Variation of elastic moduli with temperature. The elastic stiffness moduli at various temperatures, based on the reference values of Table II, are given in Table IV. The c_{44} moduli are based on the average of the two c_{44} moduli of Table II. The given c_{13} moduli are the weighted mean of the two values computed at each temperature. Table IV gives the moduli at the highest temperature at which measurements were made and the moduli at the temperatures of the Ti and Zr phase transformations as extrapolated, where necessary. Figures 3, 4, and 5 show the curves obtained from plotting the results given in Table IV. All of the c_{11}, c_{33}

TABLE IV. Stiffness moduli of Ti, Zr, and Hf at various temperatures (10^{12} dyn/cm^2).

Temp. °K	c_{11} Ti	Zr	Hf	c_{33} Ti	Zr	Hf	c_{44} Ti	Zr	Hf	$c_{66}=\frac{1}{2}(c_{11}-c_{12})$ Ti	Zr	Hf	c_{13} Ti	Zr	Hf	c_{12} Ti	Zr	Hf
4	1.761	1.554	1.901	1.905	1.725	2.044	0.508	0.363	0.600	0.446	0.441	0.578	0.683	0.646	0.655	0.869	0.672	0.745
23	1.759	1.553	1.900	1.905	1.725	2.043	0.508	0.362	0.599	0.446	0.440	0.578	0.682	0.646	0.655	0.867	0.673	0.744
73	1.749	1.542	1.891	1.894	1.716	2.035	0.505	0.358	0.595	0.439	0.432	0.572	0.680	0.648	0.658	0.871	0.678	0.747
123	1.726	1.522	1.875	1.876	1.702	2.022	0.499	0.351	0.588	0.425	0.418	0.562	0.681	0.648	0.659	0.877	0.685	0.751
173	1.699	1.495	1.859	1.857	1.687	2.008	0.490	0.342	0.579	0.405	0.401	0.551	0.684	0.648	0.660	0.889	0.692	0.757
223	1.668	1.470	1.842	1.837	1.672	1.993	0.481	0.333	0.571	0.384	0.383	0.539	0.687	0.649	0.661	0.901	0.705	0.765
273	1.639	1.445	1.822	1.816	1.655	1.977	0.472	0.324	0.562	0.363	0.363	0.526	0.689	0.651	0.661	0.913	0.719	0.770
298	1.624	1.434	1.811	1.807	1.648	1.969	0.467	0.320	0.557	0.352	0.353	0.520	0.690	0.653	0.661	0.920	0.728	0.772
323	1.609	1.420		1.795	1.639		0.462	0.316		0.342	0.343	0.513	0.691	0.653		0.925	0.734	
373	1.579	1.396		1.774	1.623		0.453	0.308		0.323	0.325	0.500	0.694	0.654		0.934	0.746	
423	1.551	1.370		1.753	1.607		0.444	0.301		0.304	0.307	0.486	0.695	0.654		0.943	0.756	
473	1.522	1.347		1.734	1.591		0.434	0.295		0.285	0.290	0.472	0.695	0.654		0.952	0.767	
523	1.495	1.323		1.715	1.574		0.424	0.288		0.267	0.273	0.458	0.692	0.656		0.961	0.778	
573	1.468	1.301		1.696	1.559		0.414	0.282		0.250	0.257	0.443	0.692	0.657		0.967	0.786	
623	1.442	1.278		1.678	1.543		0.403	0.276		0.234	0.243	0.428[a]	0.691	0.658		0.973	0.793	
673	1.416	1.257		1.661	1.526		0.392	0.270		0.219	0.229		0.690	0.659		0.978	0.799	
723	1.392	1.235		1.644	1.510		0.381	0.264		0.205	0.215		0.692	0.659		0.983	0.806	
773	1.368	1.214		1.627	1.493		0.370	0.257		0.191	0.201		0.688	0.659		0.985	0.812	
823	1.345	1.192		1.610	1.476		0.359	0.251		0.178	0.188		0.688	0.659		0.988	0.816	
873	1.322	1.168		1.593	1.460		0.348	0.245		0.166	0.175		0.688	0.659		0.991	0.819	
923	1.299	1.147		1.576	1.443		0.337	0.239		0.154	0.162		0.688	0.658		0.992	0.824	
973	1.276	1.127		1.560	1.425		0.326	0.232		0.142	0.149			0.657		0.993	0.828	
1023	1.253	1.108		1.545	1.409		0.316	0.226		0.130	0.137			0.656		0.994	0.834	
1073	1.231	1.087		1.529	1.393		0.307	0.220		0.118	0.125			0.656		0.996	0.838	
1083				1.526														
1093								0.202						0.656				
1105					1.382						0.117						0.840	
1123	1.210	1.067					0.297			0.107						0.996		
1133		1.064			1.374[a]			0.201[a]			0.109[a]			0.656[a]			0.840[a]	
1153	1.197						0.291			0.102						0.996		
1156	1.196			1.504[a]			0.291			0.100[a]			0.688[a]			0.996[a]		

[a] From extrapolated curve.

TABLE V. Differences in cross checks at various temperatures.

Temp. °K	$\frac{(c_{44})_A-(c_{44})_C}{c_{44}}\times 100$ Ti	Zr	Hf	$\frac{\rho V_{PS}^2 \text{ obs.-calc.}}{\text{obs.}}\times 100$ Ti	Zr	Hf	$\frac{(c_{13}) \text{ from } \rho V_{QL}^2-c_{13} \text{ from } \rho V_{QS}^2}{c_{13} \text{ av.}}\times 100$ Ti	Zr	Hf
4	0.16	0.11	0.33	0.00	0.05	0.33	1.3	1.5	1.8
73	0.17	−0.11	0.33	0.13	0.25	0.32	2.6	1.5	1.2
173	0.17	−0.06	0.23	0.38	−0.11	0.33	2.0	2.5	1.3
298	0.15	0.00	0.23	−0.17	−0.03	0.11	1.3	1.4	3.0
373		0.05			+0.07			0.91	
573		0.36			+0.33			−0.15	
773		0.16			+0.55			0.45	
973		0.35			+0.53			0.15	
1073		0.35			+0.17			−0.30	

moduli are plotted, for comparison, in Fig. 3, along with the ρV_{QL}^2 for Ti and Zr. The curves for the shear moduli are given in Fig. 4, and those for the c_{12} and c_{13} moduli in the lower part of Fig. 5.

The inaccuracies in the tabulated results due to thermal expansion assumptions, errors in temperature measurements and other miscellaneous factors, are indicated by the change with temperature in the cross checks, shown in Table V. For most accurate determination of the effects of temperature on the elastic moduli, the differences should remain the same as in the reference temperature cross checks given in Table III. The c_{44} cross checks for Zr and Ti show no systematic variance at low temperatures, indicating that the assumptions in the thermal expansivities were not significantly in error. The small systematic changes in the Hf cross checks may be due to neglecting the anisotropy in expansivity. The cross checks above 298°K, which are available only for Zr, indicate that the probable errors are larger in the higher temperature region but still within the range of 0.25% for each ρV^2, again neglecting the errors in density at the reference temperature.

The variations with temperature of linear adiabatic compressibilities parallel and perpendicular to the c axes, $\beta_{\parallel}$ and $\beta_{\perp}$, respectively, and the volume compressibilities are given in Table VI and plotted in Fig. 5. They are computed from the following equations:

$$\beta_{\parallel}=\frac{c_{11}+c_{12}-2c_{13}}{c_{33}(c_{11}+c_{12})-2c_{13}^2},$$
$$\beta_{\perp}=\frac{(c_{33}-c_{13})}{c_{33}(c_{11}+c_{12})-2c_{13}^2}, \tag{5}$$
$$\beta_{\text{vol}}=2\beta_{\perp}+\beta_{\parallel}.$$

The compressibilities given for Ti at 973°K and above are based on the extrapolation of the c_{13} versus temperature curve shown in Fig. 5. Since c_{13} shows a very slight temperature dependence below 773°K, and the measured c_{13} for Zr is essentially temperature independent above 773°K, it seems justified to assume

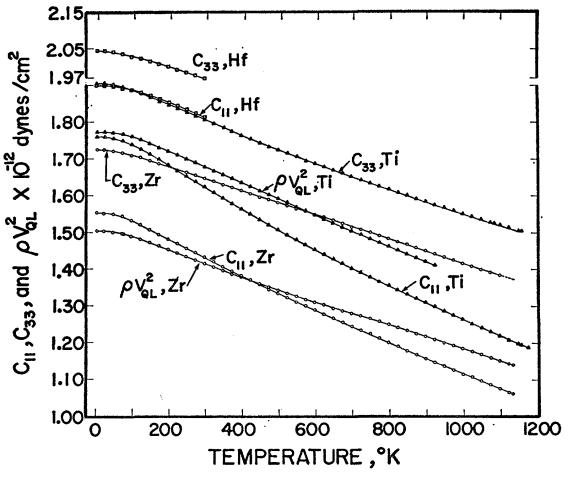

FIG. 3. Curves for c_{11} and c_{33} obtained for data of Table IV and ρV_{QL}^2 measurements for Ti and Zr. ρV_{QL}^2 for Hf coincides with c_{11} Hf curve.

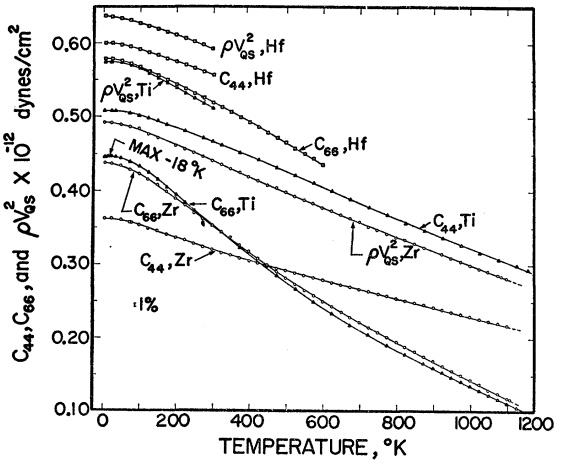

FIG. 4. Curves for c_{44} and c_{66} obtained from data of Table IV and ρV_{QS}^2 measurements.

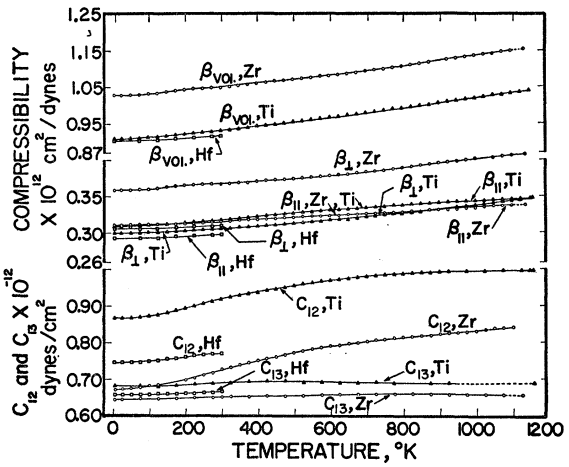

FIG. 5. Curves for adiabatic linear and volume compressibilities obtained from Table V data (upper). Curves for c_{12} and c_{13} obtained from Table IV data.

no significant decrease in accuracy of the given compressibilities between 773 and 1083°K.

Comparison of temperature dependence of the elastic moduli. The temperature coefficients for the change in elastic moduli $(1/M)(dM/dT)$, where M is any one of the elastic moduli, have a negative algebraic sign for all compressional and shear moduli at temperatures above 20°K. With exception for possible anomalous maxima in certain shear moduli in Ti, c_{66}, ρV_{QS}^2 and ρV_{PS}^2, the temperature coefficients approach zero at 4°K. The anomalous maxima are in the range of 15 to 18°K. In three repeated sets of measurements for the c_{66} mode, for example, the $(f_0)_T$ decreased by 0.05% on cooling from 18 to 2°K and increased correspondingly upon subsequent heating. Although this magnitude of change is within the probable error of $(f_0)_T$ measurements, a reproducible systematic change of this nature cannot be explained on the basis of fluctuating conditions. It appears then that c_{66} for Ti reaches a maximum at 18°K and has a positive temperature coefficient at 4°K.

The most interesting features of the data are:

TABLE VI. Compressibility parameters at various temperatures (10^{-12} cm²/dyn).

Temp. °K	$\beta_\perp$ Ti	$\beta_\perp$ Zr	$\beta_\perp$ Hf	β_{11} Ti	β_{11} Zr	β_{11} Hf	β_{vol} Ti	β_{vol} Zr	β_{vol} Hf
4	0.300	0.359	0.305	0.309	0.311	0.293	0.908	1.029	0.903
73	0.300	0.359	0.306	0.310	0.311	0.293	0.911	1.030	0.904
173	0.303	0.365	0.308	0.314	0.313	0.296	0.920	1.042	0.911
298	0.306	0.367	0.310	0.318	0.316	0.297	0.931	1.050	0.918
373	0.309	0.370		0.322	0.318		0.940	1.058	
473	0.313	0.374		0.326	0.321		0.951	1.069	
573	0.316	0.377		0.330	0.324		0.963	1.078	
673	0.321	0.382		0.334	0.325		0.975	1.090	
773	0.326	0.387		0.337	0.328		0.988	1.102	
873	0.331	0.394		0.340	0.329		1.001	1.118	
973	0.336[a]	0.400		0.343[a]	0.333		1.016[a]	1.132	
1073	0.342[a]	0.405		0.345[a]	0.337		1.029[a]	1.146	
1135		0.407[a]			0.338[a]			1.154[a]	
1156	0.347[a]			0.346[a]			1.041[a]		

[a] Extrapolated from curves.

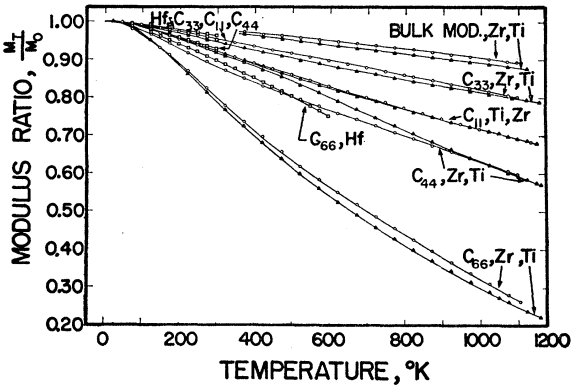

FIG. 6. A comparison of the temperature dependence of c_{11}, c_{33}, c_{44}, c_{66}, and the bulk moduli $(1/\beta_{vol})$ for Ti, Zr, and Hf. M_T/M_0 ordinate is the value of a modulus normalized to that at 4°K.

(1) the marked anisotropy in the temperature coefficients of the shear moduli for both Ti and Zr, (2) the similarities in the effects of temperature on the elastic moduli of Ti and Zr, and (3) the marked positive curvatures in certain of the modulus versus temperature plots. The first two characteristics are best shown by the normalized moduli M_T/M_0, where M_T is the modulus at a temperature T and M_0 is the modulus at 4°K. Figure 6 gives the M_T/M_0 versus temperature curves for the moduli c_{11}, c_{33}, c_{44}, and c_{66}. The curves for the computed bulk moduli of Ti and Zr are included for comparison. It is immediately evident that the c_{66} shear moduli for Ti and Zr are by far the most temperature sensitive, decreasing by about 75% between 4°K and the respective phase-transformation temperatures. The c_{44} shear moduli for Ti and Zr are the next most temperature sensitive, with a total decrease of about 42%. The anisotropy is again evident in the compressional moduli of Ti and Zr where the c_{11} decrease

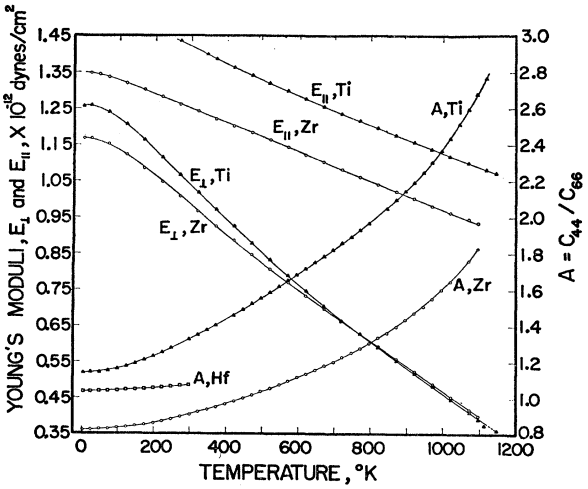

FIG. 7. Temperature dependence of the directional Young's moduli, $E_{||}$ (c axis) and $E_\perp$ (90° to c axis), and shear modulus anisotropy ratio $A = c_{44}/c_{66}$ for Ti, Zr, and Hf, as computed from data of Table IV.

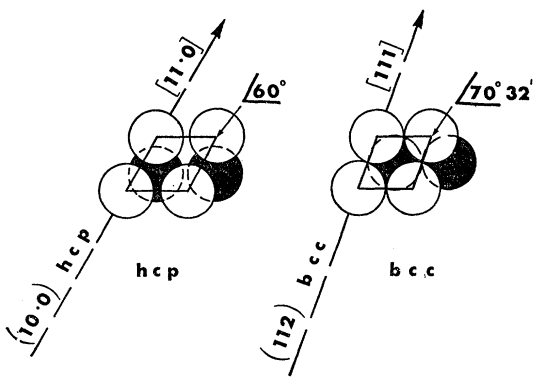

FIG. 8. Atomic projections on {000·1} hcp planes and {110} bcc showing changes in packing sublattice to relations and crystallographic directions which result from Burger's hcp ⇄ bcc transformation scheme. Shear systems for each lattice are indicated.

by 32% compared to 21% for the c_{33}. The bulk moduli, for comparison, decrease by about 12%. The Hf results give a similar type of anisotropy in the range of 4–300°K, although the differences in the temperature sensitivities are not so marked. In all three metals the ratios c_{44}/c_{66} and c_{33}/c_{11} increase with increasing temperature. The shear modulus ratios $A=c_{44}/c_{66}$ are plotted in Fig. 7. The positive deviations from linear modulus versus temperature curves above 200°K for Ti and Zr are most significant for the c_{66} moduli, beginning at approximately 420°K, and are also evident in the c_{11} curves and the c_{44} curve for Zr.

The effects of temperature on the computed Young's moduli, $E_\perp$ and $E_{||}$, show an interesting comparison (Fig. 7). At 4°K the $E_\perp$ for Zr and Ti differ by about 10%, whereas, at 1100°K the difference is about 1%. In both metals the decrease in $E_\perp$ is very large, 67% for Ti and 64% for Zr, due to the influence of the c_{66} shear modulus on the computation

$$E_\perp=\frac{2c_{66}[c_{33}(c_{11}+c_{12})-2c_{13}^2]}{c_{11}c_{33}-c_{13}^2}. \quad (6)$$

The changes in $E_{||}$ with temperature are strikingly similar for Ti and Zr, both decreasing by about 30% between 4 and 1100°K. $E_{||}$ for Ti is about 15% larger than $E_{||}$ for Zr at 4°K.

The modulus versus temperature curves for Hf in the range of 4–300°K, all show definite negative curvatures. The c_{66} curve for Hf has a strong negative curvature between 300 and 600°K, in marked contrast to the curves for c_{66} in Ti and Zr.

DISCUSSION

Relation of Shear Modulus Data to the Phase Transformations in Zr and Ti

The phase transformations in Ti and Zr have been shown to be of the classical diffusionless character involving very small volume changes (<1%) and very simple lattice relationships.[7] The bcc structure cannot be retained on cooling, but a remarkable orientation relationship persists between hcp and bcc grains on thermal cycling through the transformation.[24] Burgers[7] concluded that the {00·1} planes of the hcp phase of Zr become {110} planes of the bcc phase and showed that this relationship can be accomplished by a primary shear displacement along {10·0} prism planes of the hcp phase in a ⟨11·0⟩ direction as shown schematically in Fig. 8. The corresponding reverse shear system in the bcc phase is {112}⟨111⟩. Small dilatation strains are necessary to complete the structural change.

This proposed transformation mechanism has been verified somewhat by habit planes observed in hcp Ti, which fall within 10° of the {10·0} prism planes.[8] The present elastic moduli are probably more conclusive verification since the shear modulus involved in {10·0}⟨11·0⟩ shear is precisely the c_{66} modulus, which is markedly smaller in magnitude than the shear modulus for other principal shear systems in either hcp metal at the respective transformation temperatures. Since the structural forces opposing a phase transformation, i.e., the interfacial surface energy and the strain energy for displacement, are directly related to the shear modulus, the relatively small c_{66} may explain the preference for Burgers' mechanism.

Further evidence for this shear mechanism is indicated in the fact that the c_{66} moduli in Ti and Zr are remarkably coincident in magnitude at the transformation temperatures, whereas all other principal elastic moduli differ by more than 10%. Kaufman estimates that the chemical driving force for the Zr and Ti transformations, $\Delta F^{\alpha\to\beta}$, have remarkably similar temperature dependence and magnitude at their respective transformation temperatures.[25] The opposing forces would then be expected to be similar in order for the transformation temperatures to coincide within 20°K.

Significance of the Temperature Dependence of c_{66}

Existing theories for the temperature dependence of elastic moduli offer no obvious explanations for either the large temperature dependence of the c_{66} moduli in Ti and Zr nor the remarkably similar values of these two moduli between 4 and 1130°K. There are, however, sufficient data in the literature which permits a comparison of our data with elastic modulus data in a number of other hcp metals. Table VII lists all of the hcp metals in order of decreasing c/a ratio at 300°K and certain properties pertaining to the interpretation of the elastic modulus data. The sources of the data are indicated in the table (see Refs. 26–37). The fifth

[24] J. W. Glen and S. F. Pugh, Acta Met. **2**, 520 (1954).
[25] L. Kaufman, Acta Met. **7**, 575 (1959).
[26] W. B. Pearson, *Handbook of Lattice Spacings and Structures of Metals* (Pergamon Press, Inc., New York, 1958).
[27] R. J. Wasilewski, Trans. AIME **221**, 1081 (1961).

TABLE VII. Correlation of c/a ratio in hcp metals with occurrence of phase transformation and temperature dependence of elastic shear moduli.

Metal	c/a at 300°K	a_0(Å)	Sign of $\frac{\Delta c/a}{\Delta T}$	Temp. (°K) hcp → bcc transformation	$-10^6\times\left(\frac{1}{M}\frac{\Delta M}{\Delta T}\right)$ at 300°K c_{66}	c_{44}	References Elastic moduli	Other data
Cd	1.88	2.973	+	···	867	844	31	26
Zn	1.86	2.660	+	···	538	750	32	26
Co	1.623	2.50	+	···	330	412	33	26
Mg	1.623	3.203	+	···	462	533	34	26
Re	1.615	2.76	−	···	···	···		27
Tc	1.60	2.735	?	?	···	···		26
Tl	1.598	3.50	+	507	887	231	35	26
Sc	1.594	3.308	+	1608	···	···		28
Zr	1.593	3.23	+	1135	1000	523	a	17
Gd	1.590	3.63	+	1535	···	···		28
Ti	1.587	2.95	+	1155	1000	380	a	14
Lu	1.583	3.505	+	1600	···	···		28
Tb	1.583	3.599	+	1583	···	···		28
Ru	1.582	2.70	+	···	···	···		26
Hf	1.581	3.19	+	~2000	476	325	a	26
Os	1.579	2.73	+	···	···	···		26
Dy	1.574	3.592	+	1670	···	···		28
Y	1.572	3.645	+	1760	413	333	36	28
Tm	1.572	3.537	+	···	···	···		28
Er	1.571	3.559	+	···	···	···		28
Ho	1.571	3.576	+	1715	···	···		28
Be	1.568	2.281	−	1523	196	184	37	26,29
Li	1.564	3.086		70	···	···		30

[a] Present data.

column of Table VII lists the temperatures of the hcp → bcc transformations, where evidence exists for their occurrence. Among the 17 metals with $c/a<1.60$ such evidence has been found in all but four, the exceptions being Ru, Os, Tm, and Er. The former two metals also have relatively small a_0 parameters (column 3), thus possibly accounting for the relative stability of the hcp structures. Columns 6 and 7 of Table VII contain the temperature coefficients, $-(1/M)(\Delta M/\Delta T)$, of the principal elastic shear moduli evaluated at 300°K. For Cd, Zn, Co, and Mg, in which bcc phases are not found, the c_{44} shear moduli have equal or greater temperature dependence than c_{66}. For c/a between 1.60 and 1.57, however, c_{66} has a singificantly greater temperature dependence than c_{44}, with the difference at 300°K having some direct correlation with the temperature of the phase transformation. Be, with $c/a<1.57$, has unusually small temperature coefficients in its elastic properties and is also unusual with respect to thermal expansion, i.e., c/a shows a negative dependence on temperature, whereas all other hcp metals with $c/a<1.60$ show a positive dependence.

An explanation for the apparent change in the temperature dependence of c_{44}/c_{66} with the c/a ratio is suggested by the fact the $c/a<$ideal implies a larger separation of the atoms in the basal planes of the hcp structure than exists between atoms in different sublattices, as shown schematically in Fig. 8 where the two hexagonal sublattices are represented by light and dark atoms respectively. Because of wider separation of the atoms within a basal plane it may be assumed that thermal energy is most likely to first excite those vibrational modes which change these separations. Since shear distortions are easier to produce than compressional distortions, which change the volume of the structure, the thermal modes corresponding to the c_{66} shear mode probably contribute most to the displacement amplitudes. The large temperature dependence of the c_{66} shear modulus is then a result of the dependence of the elastic modulus on the thermal energy taken up by this mode, in accordance with the more generalized theories of Zener and others regarding the effect of temperature on elastic moduli.[5] Because the c_{66} shear displacements may involve a change in the direction of the interlattice bonds the ease of exciting these displacements should be also dependent on the energy needed to change bond directions, which in turn could account for the differences observed among the metals with $c/a<1.60$.

[28] F. H. Spedding, J. J. Hanak, and A. H. Daane, J. Less-Common Metals **3**, 110 (1961).
[29] A. J. Martin and A. Moore, J. Less-Common Metals **1**, 85 (1959).
[30] C. S. Barrett, *Phase Transformations in Solids* (John Wiley & Sons, Inc., New York, 1951), Chap. 13.
[31] C. W. Garland and J. Silverman, Phys. Rev. **119**, 1218 (1960).
[32] G. A. Alers and J. R. Neighbours, Phys. Chem. Solids **7**, 58 (1958).
[33] H. J. McSkimin, J. Appl. Phys. **26**, 405 (1955).
[34] L. J. Slutsky and C. W. Garland, Phys. Rev. **107**, 972 (1957).
[35] R. W. Ferris, M. L. Shepard, and J. F. Smith, J. Appl. Phys. **34**, 768 (1963).
[36] c_{44} and c_{66} are reversed in this reference: J. F. Smith and J. A. Gjevre, J. Appl. Phys. **31**, 645 (1960).
[37] J. F. Smith and C. L. Arbogast, J. Appl. Phys. **31**, 99 (1960).

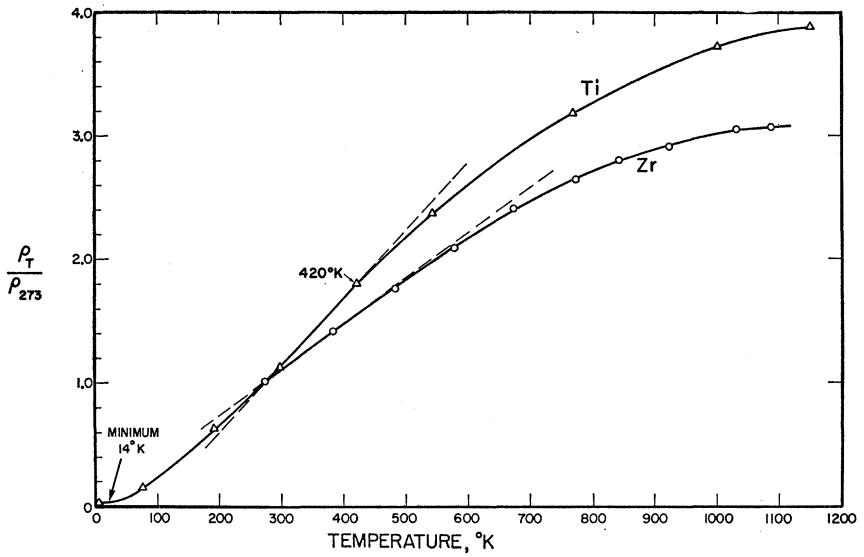

FIG. 9. Electrical resistivity normalized to that at 273°K as a function of temperature from data given in Refs. 38 and 39. Dashes are extensions of linear portions of curves.

Phase transformations and the c/a ratio. The apparent systematic relationship between the occurrence of the hcp → bcc phase transformations among hcp metals and the c/a ratio may not be related to the temperature dependence of the elastic moduli. Measurements of the elastic moduli in Ru and/or Os should be helpful in deciding this question. At present, however, there are several bits of evidence which suggest that the two phenomena are related through the anharmonic contributions to the vibrational free energy of the hcp structures at high temperatures. Most of the hcp metals which have transformations, including Ti and Zr, show a marked positive temperature dependence of the c axis thermal expansion coefficients at high temperatures. This phenomenon may be interpreted as a result of interatomic repulsive forces created by the large vibrational amplitudes associated with the c_{66} transverse thermal modes. Since the two sublattices may not be vibrating in phase the repulsive forces will increase with amplitudes of vibration. The onset of positive curvature in the c_{66} versus temperature curves at 420°K (Fig. 4) can then be interpreted as a decreasing effect of temperature on the vibrational amplitudes. The same conclusion can be obtained from a qualitative analysis of the electrical resistivity data for both Ti and Zr,[38,39] shown in Fig. 9. In both sets of data the negative departure from a linear dependence begins at approximately 420°K, which corresponds remarkably well with the onset of anomalous curvature in the c_{66} curves. If it is assumed that the resistance anomaly is due to changes in the electron scattering probability by the lattice, then we reach the same conclusion as stated above, implying a gradual increase in the effective Debye θ above 420°K.

This assumption implies that the electrical resistance is closely associated with the transverse thermal vibrations in Ti and Zr and is, consequently, a deviation from the Bloch theory of conductivity, which assumes that conduction electrons are scattered only by longitudinal phonons.[40] The latter assumption, however, is inconsistent with the fact that Debye θ computed from electrical resistance data do in many cases agree with those computed from the average wave velocities obtained from all the elastic moduli. Blackman[41] suggests that the Debye θ agreements indicate that all thermal waves contribute to the electrical resistance.

The effect of anharmonicity on the thermodynamic properties can be quantitatively estimated using the expansion of the potential energy in terms of powers of the lattice displacements due to thermal motion, as treated by Born and Brody[42]:

$$E(x)=ax^2+bx^3+cx^4+\cdots, \tag{7}$$

where x is the atomic displacement from the equilibrium interatomic distance. Neglecting higher than fourth power terms the thermodynamic free energy is approximated as

$$F=F^h-3RBkT^2=F^h-\tfrac{1}{2}T(C_V-C_V{}^h), \tag{8}$$

where R and k are the gas and Boltzman constants, respectively, and F^h and $C_V{}^h$ are the free energy and specific heat at constant volume in the harmonic approximation. The quantity B represents the coefficients of the anharmonic terms of Eq. (7) and can be evaluated in terms of C_V as deduced from measured C_P data, since $C_V{}^h$ is the lattice specific heat evaluated from the Debye approximation. The C_V to be used here is that

[38] J. L. Wyatt, Trans. AIME **197**, 903 (1953).
[39] L. A. Cook, L. S. Castleman, and W. E. Johnson, Westinghouse Corporation Report WAPD-25, 1950 (unpublished).
[40] F. Bloch, Z. Physik **52**, 555 (1928).
[41] M. Blackman, in *Handbuch der Physik*, edited by S. Flügge (Springer-Verlag, Berlin, 1955) Vol. VII, Part 1, p. 379.
[42] M. Born and E. Brody, Z. Physik **6**, 132 (1921).

which arises from the lattice vibrations only; consequently, besides the uncertainties involved in the C_P data and the C_P-C_V correction, the electronic contribution C_E adds further question to the computation of the lattice C_V. Nevertheless, Figs. 10 and 11 show the results of an attempt to evaluate the lattice C_V, i.e., (C_V-C_E), for Ti and Zr, respectively, from what was considered to be the C_P data most representative of the pure metals.[43] The spread among the available sets of C_P measurements for both Ti and Zr is very large, and in all cases the data above 1000°K seem to contain contributions from the latent heat associated with the phase transformations; consequently, the C_V computations were carried out only to 1000°K using the relation

$$C_V=\left(\frac{\beta}{\alpha^2VT+\beta C_P}\right)C_P^2, \tag{9}$$

where β is the adiabatic volume compressibility obtained from the present elastic constant data, α is the coefficient of volume thermal expansion, and V is the specific volume. The negative curvature in C_V for Ti above 800°K arises from the unusual temperature dependence of α indicated in the dilatation data from which α was computed.[21] The negative slope would be much greater in magnitude if the x-ray data[14] were used.

The variation of the electronic specific heat C_E with temperature for Ti and Zr was obtained from the computations of Shimizu *et al.*[44,45] in which the Fermi-Dirac integrals are evaluated at high temperatures. According to these computations, the electronic specific heat coefficients γ increase with temperature from a value of $\sim 8\times10^{-4}$ cal/deg^2 mole at 0°K to about 12.5×10^{-4} cal/deg^2 mole above 500°K for Ti and 6.7×10^{-4}–14×10^{-4} cal/deg^2 mole for Zr between 0 and 1100°K.

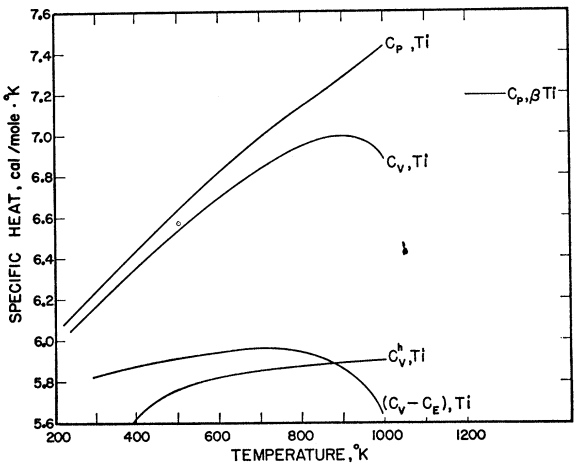

FIG. 10. Temperature dependence of C_P for Ti (measured by Scott), C_V (computed from Eq. 9), C_V-C_E (computed from C_E calculations of Shimizu), and C_V^h (determined from table of C_V^h versus θ/T using Debye θ_E values of Table VIII).

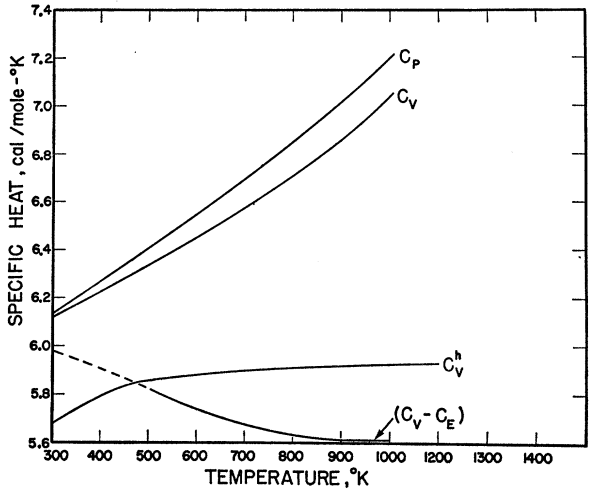

FIG. 11. Temperature dependence of C_P, C_V, C_V-C_E, and C_V^h for Zr, from sources indicated in Fig. 10 caption.

Because of the considerable uncertainties discussed above, we cannot place too much confidence in the magnitude of the differences between (C_V-C_E) and C_V^h. The temperature dependence of (C_V-C_E) indicates, however, that the effect of the anharmonicity on the vibrational free energy becomes less negative as the temperature increases, and eventually, in the range of 900°K, there is actually a positive contribution, which increases the lattice free energy above that of the harmonic approximation.

Thus, there seems to be sufficient grounds for a more thorough study of the assumption that the instability of the hcp structures relative to the bcc structures in Ti and Zr above the respective transformation temperatures results from the effects of the anharmonicity on the vibrational frequency spectrum of the hcp structure. When this interpretation is considered in terms of Burgers' model for the structural change and Zener's explanation of the high-temperature stability of the bcc phase,[5] the transformation can be viewed as a sudden shift in the direction of the high-amplitude thermal vibrations. The atoms of the formerly hexagonal basal plane are suddenly brought together in the close packed {110} planes of the bcc phase, as shown in Fig. 8b, thereby decreasing the amplitudes of the formerly c_{66} modes of the hcp phase. The large amplitudes modes in the bcc phase are presumably the {110}⟨110⟩ shear displacements which correspond in direction to the formerly c_{44} modes of the hcp structure. The increase in entropy associated with the transition represents, then, the greater freedom for the {110}⟨110⟩ thermal vibrations in the bcc structure.

As mentioned in the introduction to this paper, the habit-plane studies in Ti and Zr argue against the presumed anisotropy of bcc shear moduli. Conse-

[43] J. L. Scott, Oak Ridge National Laboratory Report ORNL-2328, 1957 (unpublished).
[44] M. Shimizu, J. Phys. Soc. Japan **18**, 1192 (1963).
[45] M. Shimizu, calculations for Zr by private communication.

quently, a more explicit treatment of the change in vibrational modes accompanying the phase transformation requires measurements of the elastic moduli in bcc crystals representing the Ti-Zr structures.

The Low-Temperature Anomaly in Ti

The indications of a maximum in the c_{66} shear modulus in Ti at about 18°K are discussed above and indicated in Fig. 4. In view of the small deviations from normal curvature these observations would indicate only a small probability of anomalous properties in Ti at this temperature. Recently, however, an anomalous minimum in the electrical resistance of relatively pure Ti was reported at about 14°K.[46] Here again the deviation from the normal resistivity curve was very small, and the authors attributed their observations to possible impurity effects, since the intentional addition of certain transition metal impurities tended to increase the deviation.

The explanation of the resistivity minimum was based on current theories which require the presence of localized magnetic moments in Ti alloys. This explanation would not hold for pure Ti in which localized moments are presumed not to exist. It seems that studies of the temperature dependence of the shear moduli in Ti-Mn single crystals would be helpful in explaining the observed maximum reported here, since these alloys showed pronounced resistivity minima.[46]

Debye θ at 4°K

The Debye θ temperatures computed from the 4°K elastic moduli, θ_E, are given in Table VIII. These values are based on mean wave velocities determined from Wolcott's tables[47] and unit cell volumes computed from the lattice parameters given in Refs. 14–16, for Ti, Zr, and Hf, respectively. Mean wave velocities were also determined from the isotropic bulk and rigidity moduli using the Voigt and Ruess approximations, as suggested by Anderson.[48] This latter method gives Debye θ values which are within 0.5° of those given in Table VIII. The Debye θ computed from specific heat data, $\theta_{S.H.}$, by Kneip *et al.*[49] are also given in Table VIII. The $\theta_{S.H.}$ for Hf+8 at.% Zr was computed from the reported $\theta_{S.H.}$ for Hf+(0.05 wt% Zr) assuming a linear dependence of θ with composition. More recent specific heat measurements in Hf-Zr alloys confirm the linear dependence.[50]

TABLE VIII. Comparison of Debye θ computed from 4°K elastic moduli with specific heat θ of Kneip, *et al.* (Ref. 49).

	θ_E	$\theta_{S.H.}$
Titanium	425.65°	428 ±5°
Zirconium	295.98°	291.7±1.3°
Hf+8 at.% Zr	256.29°	255.5[a]

[a] Interpolation from 252±1° for pure Hf assuming a linear dependence on Zr concentration.

The agreement between θ_E and $\theta_{S.H.}$ is remarkably good especially when one considers the discrepancies which exist in the corresponding data for all other hexagonal metals. The discrepancies are greater than 20° for Mg, Zn, and Cd (See Refs. 34, 32, and 31) and greater than 200° for Be.[37] Since it now seems clear that θ_E and $\theta_{S.H.}$ should agree,[41] the present agreement has no significance except to more firmly establish theoretical arguments and to verify the interpretation of the specific heat data.

Note added in proof: Recent measurements by the present authors of the temperature dependence of c_{66} and c_{44} in single crystals of Ru between 70 and 300°K give temperature coefficients (see Table VII) of −167 and −213 ppm/°K, respectively. Although the c/a ratio for Ru is <1.62, the hcp → bcc transformation does not occur in the pure metal; these results, then, tend to confirm the supposition that a direct relationship exists between the occurrence of this transformation and the relative magnitudes of the temperature coefficients of the hcp shear moduli.

ACKNOWLEDGMENTS

R. E. Black and A. Sather assisted in the crystal preparation and the measurements of acoustic wave velocities. We thank L. T. Lloyd for careful editing of the manuscript and Dr. M. Shimizu for communicating his electronic specific heat calculations before publication.

This research was carried out under the auspices of the U. S. Atomic Energy Commission.

APPENDIX

The equation for the stiffness modulus for (112)[111] shear in a cubic crystal is

$$c_{(112)[111]}=\tfrac{1}{3}(c_{11}-c_{12}+c_{44})$$

which is a minimum relative to the 2 principal shear moduli, c_{44} and $\frac{1}{2}(c_{11}-c_{12})$, when $2c_{44}/(c_{11}-c_{12})=1$. From the point of view of the shear modulus, shear on (112)[111] is most favored in an isotropic bcc crystal.

[46] R. R. Hake, D. H. Leslie and T. G. Berlincourt, Phys. Rev. **127**, 170 (1962).
[47] N. M. Wolcott, J. Chem. Phys. **31**, 536 (1959).
[48] O. Anderson, Phys. Chem. Solids **24**, 909 (1963).
[49] G. D. Kneip, Jr., J. O. Betterton, Jr., and J. A. Scarborough, Phys. Rev. **130**, 1687 (1963).
[50] J. O. Betterton, Jr. (private communication).